

# ON THE PROBLEMS OF RIBLETS AS A DRAG REDUCTION DEVICE

G. ARUMUGAM

*INRIA, F-78153 Le Chesnay, France and University of Madurai, India*

AND

O. PIRONNEAU

*University of Paris 6, Paris and INRIA, Domaine de Voluceau, Rocquencourt,  
B.P. 105, F-78153, Le Chesnay, France.*

## SUMMARY

Some recent experiments have shown that it is possible to reduce the drag of a body in a uniform flow by digging tiny ribs or 'riblets' on its skin. This paper deals with (i) the formulation of the problem into a distributed parameter optimum design problem and (ii) with its numerical solution by the finite element method and the techniques of optimal control. Some numerically optimal riblets are presented.

**KEY WORDS** Fluid dynamic drag reduction Riblets Optimal distributed parameter systems Optimal shape design

## 1. INTRODUCTION

Some recent experiences on sailing boats (the *Stars and Stripes*) and airplanes have shown that their aerodynamics can be improved to some extent by digging tiny strips, called riblets, on their body in the direction of the flow. Typically, these riblets have thickness and width less than a millimetre. Walsh<sup>1</sup> investigated experimentally the drag reduction that could be expected on a flat plate and found it to be around 5% for saw tooth-shaped riblets of height 1/30th of the boundary layer thickness and period twice its height.

The explanation of this phenomenon is not clear yet in the sense that it is not known whether it is a laminar or a turbulent phenomenon. Since the riblets are very small, they lie well inside the laminar boundary layer, and therefore *a priori* one could correlate the phenomenon to Poiseuille flow. The aim of this paper is to elucidate this last point: could the drag of a flat plate in a plane Poiseuille laminar flow be improved by digging small periodic riblets on its surface in the direction of the flow?

To answer this question, we formulate it as an optimization problem with respect to the shape of the domain of a partial differential equation (optimal shape design<sup>2-5</sup>). As we shall see, however, there is a problem with the modelling of the boundary layer. Thus one should not draw dramatic conclusions too hastily from our results. Nevertheless, by using the tools of the calculus of variation in the context of optimal shape design, we are able to prove that there are indeed better shapes than the flat plate for Poiseuille flow. The analysis is based on the derivation of first- and second-order optimality conditions and the numerical solution of these

on computer. The shape obtained is not as angular as the one suggested by Walsh,<sup>1</sup> but the height-to-length ratio is comparable. The improvement predicted is much more (around 15%), probably because the displacement of the boundary layer thickness due to the riblet is not taken into account in this study. Thus although our results indicate that one does not need to invoke the capturing of turbulent bursts by riblets to explain their drag reduction effect, this study should nevertheless be completed by a numerical simulation of the full Navier–Stokes equations in the proposed geometry.

We recall in Figure 1 the characteristics of the solution  $(u, p)$  of the Navier–Stokes equation (see Appendix I for notation)

$$u_{,t} + u\nabla u + \nabla p - \nu\Delta u = 0 \quad \nabla \cdot u = 0 \quad \text{in } O \times ]0, T[ \tag{1}$$

$$u(x, 0) = u^0(x) \quad \text{in } O \quad u(x, t) = u_\Gamma(x) \quad \text{on } \partial O \times ]0, T[ \tag{2}$$

where  $\nu$  is small,  $O = C - \Sigma$  with  $C = ] -3l, 3l[ \times ] -1, 1[ \times ] -2L, L[$ ,  $\Sigma = ] -l, l[ \times \{ L \} \times [ -L, 0]$ , and  $u_\Gamma = (0, 0, -1)$  on  $\partial C$  and 0 on  $\Sigma$ .

In the laminar boundary layer, the flow is stationary in a first approximation. (In reality, the thickness  $\delta$  of the boundary layer depends slightly on the distance  $x_3$  from the leading edge of the plate.) Thus we have a flow invariant by translation in  $x_3$ , and far from the boundary  $\Sigma$  the velocity is parallel to  $x_3$ . Now the system (1), (2) becomes

$$p_{,3} - \nu u_{,11} - \nu u_{,22} = 0 \quad p_{,1} = p_{,2} = 0 \quad u_{,3} = 0 \tag{3}$$

which is

$$-\Delta_{12}u = k \quad p = kx_3\nu \tag{4}$$

Here  $k$  is a constant to be determined when we relate the solution from (4) to the flow exterior to the boundary layers.

If we dig the riblets on the surface  $\Sigma$  (see Figure 2), we could think that (4) remains valid, though it is not evident that the velocity stays parallel to  $x_3$  when  $\Sigma$  is very irregular.

With the above hypothesis, the problem turns out to be a scalar equation in two dimensions. Finally, the periodic structure of  $\Sigma$  leads one to consider only a single cell. If  $\Sigma$  is symmetric with respect to the  $x_2$ -axis (see Figure 3), then

$$\partial u / \partial x_1 = 0 \quad \text{on } S \tag{5}$$

implies that  $u$  will be periodic on  $S$ . On the boundary above  $\Omega$ , i.e. above the laminar boundary

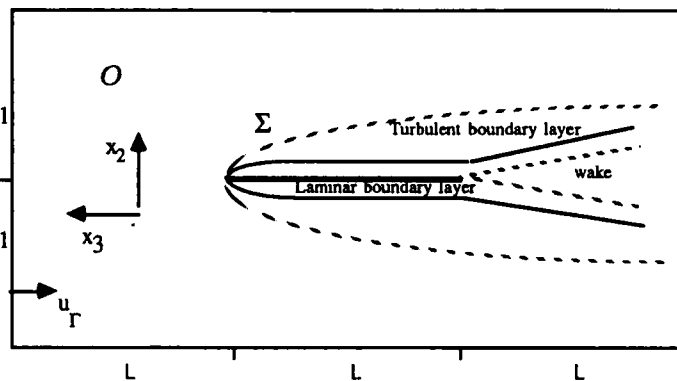


Figure 1. Characteristics of a flow around a flat plate  $\Sigma$ ; cut in the plane  $x_1 = 0$

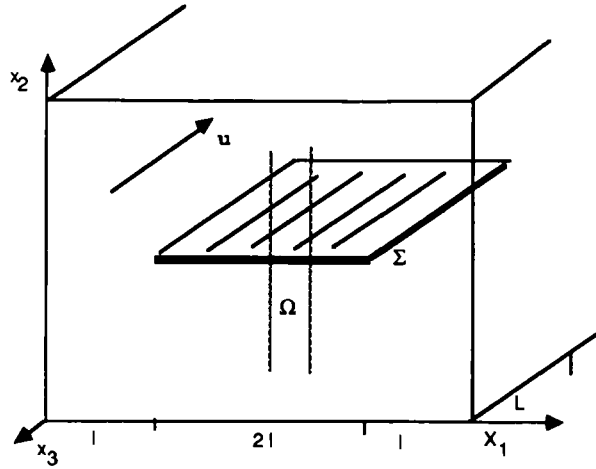


Figure 2. Geometry of the plane surface with a periodic array of riblets

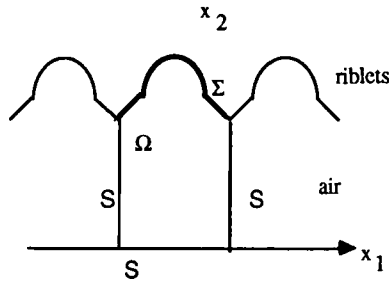


Figure 3. Computational domain; the riblets shown are those on the lower side of the flat plane of Figure 2

layer, we could assume that the flow is uniform. This we shall model by

$$\frac{\partial u}{\partial x_2} = 0 \quad (6)$$

So now the partial differential equation which determines the horizontal component of the flow,  $u(x_1, x_2)$ , is

$$-\Delta u = k \quad \text{in } \Omega \quad (7)$$

$$u|_{\Sigma} = 0 \quad \frac{\partial u}{\partial n}|_S = 0 \quad (\partial\Omega = \Sigma \cup S) \quad (8)$$

where  $k$  is the pressure gradient in  $x_3$  divided by the viscosity;  $\partial u/\partial n$  is the normal derivative of  $u$  on  $\partial\Omega$ ;  $\partial\Omega$  is the boundary of  $\Omega$ ;  $\Sigma$  is the boundary (surface) of the riblets; and  $S$  is the remaining boundary of  $\Omega$ , i.e. the vertical and the top boundaries (Figure 3).

## 2. FORMULATION OF THE OPTIMIZATION PROBLEM

The force  $dF$  that the fluid exerts on the surface element  $d\gamma$  is

$$dF = \frac{\nu}{2} \left( 0, 0, \frac{\partial u}{\partial n} \right) d\gamma \quad (9)$$

PAGE MISSING FROM 96-97

Then (with  $d$  and  $a$  given) (16)–(27) are also

$$\min_{\Sigma \in W, u \in U_d(\Omega)} \int_{\Omega} |\nabla u|^2 dx \tag{30}$$

This problem has at least one solution when  $W$  is a set of all boundaries determining  $\Omega$  in the allowable bounded open domain such that  $|\Omega| \geq a$ :

$$W = \{ \Sigma : |\Omega| \geq a, \Omega \subset O \} \tag{31}$$

For the proof, see Reference 4 Theorem 3, p.37. Let us just recall here that when (30) is minimized with respect to  $u$  with fixed  $\Omega$ , we get (7), (8) because

$$u \in U_d(\Omega), \delta u \in U_0(\gamma) \Rightarrow u + \delta u \in U_d(\Omega), u - \delta u \in U_d(\Omega)$$

Thus if  $u$  is a solution, then

$$\int_{\Omega} |\nabla u|^2 dx \leq \int_{\Omega} |\nabla(u + \delta u)|^2 dx \quad \int_{\Omega} |\nabla u|^2 dx \leq \int_{\Omega} |\nabla(u - \delta u)|^2 dx$$

which in turn implies

$$\delta \int_{\Omega} |\nabla u|^2 dx = 2 \int_{\Omega} \nabla u \nabla \delta u dx = 0, \forall \delta u \in U_0(\Omega) \Rightarrow (7), (8)$$

Uniqueness for this problem is an open question. An existence result of the same type can be proved for (23) with (31) (when  $a$  is given):

$$\max_{\Sigma \in W} \left\{ \frac{1}{|\Omega|} \int_{\Omega} |\nabla v|^2 dx : v \text{ solution of (18)} \right\} \quad W = \{ \Sigma : |\Omega| \geq a, \Omega \subset O \} \tag{32}$$

### 3.2. Optimality conditions

A. For problem (23). Let us start with simpler case (23). Let  $\Sigma$  be a solution of (23) and let  $\Omega$  be the corresponding domain. Let  $\Sigma'$ , a neighbouring boundary of  $\Sigma$  (see Figure 4), be defined by

$$\Sigma' = \{ x + \lambda \alpha(x)n(x) : x \in \Sigma \} \tag{33}$$

and let  $\Omega'$  be the corresponding domain. Here  $n(x)$  is normal to  $\Sigma$  at  $x$ ,  $\alpha(x)$  is a regular function and  $\lambda$  is a very small scalar. Let  $v^{\Omega'}$  and  $v^{\Omega}$  denote the solutions of (18) in  $\Omega'$  and  $\Omega$  respectively and let  $\delta v = v^{\Omega'} - v^{\Omega}$ . Finally, let  $S'$  be the boundary of  $\Omega' - \Sigma'$ . Now we have

$$-\Delta \delta v = 0 \quad \text{in } \Omega' \cap \Omega \quad \partial \delta v / \partial n |_{S \cap S'} = 0 \tag{34}$$

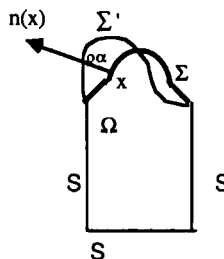


Figure 4. Local variation around an elementary riblet  $\Sigma$

But  $v^{\Omega'}(x) = v^{\Omega}(x) + \delta v(x)$  and

$$0 = v^{\Omega'}(x + \lambda \alpha n) = v^{\Omega'}(x) + \lambda \alpha \partial v^{\Omega'} / \partial n + o(\lambda) \quad \forall x \in \Sigma \quad (35)$$

Thus

$$\delta v(x) = -\lambda \alpha \partial v^{\Omega'} / \partial n + o(\lambda) \quad \forall x \in \Sigma \quad (36)$$

Therefore

$$v'_\alpha = \lim_{\lambda \rightarrow 0} \frac{v^{\Omega'} - v^{\Omega}}{\lambda} \quad (37)$$

satisfies

$$-\Delta v'_\alpha = 0 \quad \text{in } \Omega \quad v'_\alpha|_{\Sigma} = -\alpha \partial v / \partial n \quad \partial v'_\alpha / \partial n|_{\Sigma} = 0 \quad (38)$$

The criterion (23) is

$$J(\Sigma) = \frac{1}{|\Omega|} \int_{\Omega} |\nabla v|^2 dx \quad (39)$$

If  $\Sigma$  is a solution, then it has to satisfy

$$\begin{aligned} 0 \geq \delta J &= J(\Sigma') - J(\Sigma) = \frac{1}{|\Omega'|} \int_{\Omega'} |\nabla(v + \delta v')|^2 dx - \frac{1}{|\Omega|} \int_{\Omega} |\nabla v|^2 dx \\ &= \frac{1}{|\Omega'|} \int_{\Omega'} |\nabla v|^2 dx - \frac{1}{|\Omega|} \int_{\Omega} |\nabla v|^2 dx + \frac{2}{|\Omega|} \int_{\Omega} \nabla v \nabla \delta v dx + o(\lambda) \\ &= \frac{2}{|\Omega|} \int_{\Omega} \nabla v \nabla \delta v dx - \frac{\lambda}{|\Omega|^2} \int_{\Sigma} \alpha d\gamma \int_{\Omega} |\nabla v|^2 dx + \frac{\lambda}{|\Omega|} \int_{\Sigma} \alpha |\nabla v|^2 d\gamma + o(\lambda) \end{aligned} \quad (40)$$

since

$$\int_{\partial\Omega} f(x) dx = \int_{\Omega' \setminus \Omega' \cap \Omega} f(x) dx - \int_{\Omega \setminus \Omega' \cap \Omega} f(x) dx = \int_{\Sigma} \lambda \alpha f(x) d\gamma + o(\lambda)$$

That is, for all admissible  $\alpha$  we have

$$\frac{2}{|\Omega|} \int_{\Omega} \nabla v \nabla v'_\alpha dx - \frac{1}{|\Omega|^2} \int_{\Sigma} \alpha d\gamma \int_{\Omega} |\nabla v|^2 dx + \frac{1}{|\Omega|} \int_{\Sigma} \alpha |\nabla v|^2 d\gamma \leq 0 \quad (41)$$

The first integral is zero because

$$\int_{\Sigma} \nabla v \nabla v'_\alpha dx = \int_{\Omega} -\Delta v'_\alpha v dx + \int_{\partial\Omega} \frac{\partial v'_\alpha}{\partial n} v d\gamma = \int_{\Sigma} \frac{\partial v'_\alpha}{\partial n} v d\gamma = 0 \quad (42)$$

With (18), equation (41) becomes

$$\int_{\Sigma} \alpha \left| \frac{\partial v}{\partial n} \right|^2 d\gamma \leq \frac{\int_{\Sigma} \alpha d\gamma}{|\Omega|} \int_{\Omega} |\nabla v|^2 dx \quad \forall \alpha \text{ admissible} \quad (43)$$

In particular, if  $W$  is given by (28) with  $O$  sufficiently large, the set of admissible  $\alpha$  is  $\{\alpha: \int_{\Sigma} \alpha d\gamma = 0\}$  and (43) implies that  $|\partial v / \partial n|$  is constant on  $\Sigma$ .

The previous computation is somewhat formal but can be justified with regularity assumptions on  $\Sigma$  and  $v$ , either directly<sup>4</sup> or via the mapping technique of Murat and Simon.<sup>3</sup> (See also Cea and Haug<sup>2</sup> and Zolezio<sup>5</sup>.) Let us sum up the results in the following proposition.

*Proposition 2.* If  $\Sigma$  is a regular solution of (23) with (27) such that  $v$  is in  $H^2(\Omega)$ , then

$$|\partial v/\partial n| = \text{constant} \quad \text{on } \Sigma \quad (44)$$

*B.* For problem (16). We can do the same calculation on (16):

$$\begin{aligned} 0 \leq \delta J &= \frac{1}{d|\Omega'|} \int_{\Omega'} |\nabla u^{\Omega'}|^2 dx - \frac{1}{d|\Omega|} \int_{\Omega} |\nabla u^{\Omega}|^2 dx \\ &= \frac{1}{d|\Omega|} 2 \int_{\Omega} \nabla u \nabla \delta u dx - \frac{\lambda}{|\Omega|} \int_{\Sigma} \alpha d\gamma \int_{\Omega} |\nabla u|^2 dx + \lambda \int_{\Sigma} \alpha |\nabla u|^2 d\gamma + o(\alpha\lambda) \end{aligned} \quad (45)$$

From (7), (8) we deduce

$$-\Delta \delta u = \delta k \quad \delta u|_{\Sigma} = -\lambda\alpha \partial u/\partial n \quad \partial \delta u/\partial n|_{\Sigma} = 0 \quad \int_{\Omega} \delta u dx = 0 \quad (46)$$

Thus

$$\int_{\Omega} \nabla u \nabla \delta u dx = - \int_{\Omega} \delta u \Delta u dx + \int_{\partial\Omega} \delta u \frac{\partial u}{\partial n} d\gamma = -\lambda \int_{\Sigma} \alpha \left( \frac{\partial u}{\partial n} \right)^2 d\gamma$$

and (45) becomes

$$0 \leq - \int_{\Sigma} \alpha \left( \frac{\partial u}{\partial n} \right)^2 d\gamma - \frac{1}{|\Omega|} \int_{\Sigma} \alpha d\gamma \int_{\Omega} |\nabla u|^2 dx \quad \forall \alpha \text{ admissible} \quad (48)$$

*Proposition 3.* If  $\Sigma$  is a regular solution of (16), (27), then

$$|\partial u/\partial n|_{\Sigma} = \text{constant} \quad (49)$$

### 3.3. Search for an analytic solution

In both of the above cases, the problem is to find, for some given constant  $c$ , a domain  $\Omega$  such that

$$-\Delta u = k \quad u|_{\Sigma} = 0 \quad \partial u/\partial n|_{\Sigma} = c \quad \partial u/\partial n|_{\Sigma} = 0 \quad (50)$$

with  $k$  such that  $\int_{\Omega} u dx = d$  or  $k = 1$ . Note before going any further that any stationary point of (30), local maxima included, will satisfy (50); therefore the sign of the second derivative of (30) must be checked to see whether we have a local minimum or a local maximum.

One trivial solution of the problem is the flat plate. In fact, if  $\Omega = ]-l, l[ \times ]0, L[$ , then the solution of (50) is  $u = -3d/4lL^3(x_2^2 - L^2)$  corresponding to  $c = -3d/2lL^2$ , which gives the drag

$$D_p = \frac{3}{2L^2} dv = \frac{3}{2l^2} \left( \frac{1}{L} \right)^2 \quad (51)$$

There is another trivial solution of the problem (50), namely the semi-cylinder. If  $\Omega = \{x: |x| < l, x_2 < 0\} S \neq \emptyset$ , then (50) rewritten in polar co-ordinates admits a solution

$$u(r, \theta) = (-4d/\pi l^4)(r^2 - l^2)$$

with  $c = -8d/\pi l^3$  and the drag

$$D_c = 4dv/l^2 \quad (52)$$

Since  $|\Omega|$  has to be the same in both the above cases, we have  $l/L = 4/\pi$ . Thus  $D_p/D_c = 6/\pi^2 \approx 0.6$ , which says that the flat plate is 40% better than the semi-cylinder. Therefore the semi-cylinder is only a stationary point of the problem (14) and not a minimum.

To find out whether a flat plate is a minimum, we must calculate the second derivative of the criterion  $J$  with respect to  $\alpha(x)$ , i.e. calculate  $d^2 J/d\lambda^2|_{\lambda=0}$ . If this quantity is positive, then  $J$  is locally convex with respect to  $\alpha$ . Let us do this calculation for (23) with (28).

If  $v^{\Omega'} = v^{\Omega} + \lambda v'_{\alpha} + \lambda^2/2 v''_{\alpha\alpha}$ , then

$$\begin{aligned} J''_{\lambda\lambda} = \frac{d^2}{d\lambda^2} \int_{\Omega(\lambda)} |\nabla v(\lambda)|^2 dx &= 2 \int_{\Omega} |\nabla v'_{\alpha}|^2 dx + 2 \int_{\Omega} \nabla v \nabla v''_{\alpha\alpha} dx \\ &+ \frac{d^2}{d\lambda^2} \int_{\Omega(\lambda)} |\nabla v|^2 dx + 4 \int_{\Sigma} \alpha \nabla v'_{\alpha} \nabla v d\gamma \end{aligned} \quad (53)$$

However (see Appendix II),

$$\frac{d^2}{d\lambda^2} \int_{\Omega(\lambda)} |\nabla v|^2 dx = \int_{\Sigma} \alpha^2 \frac{\partial |\nabla v|^2}{\partial n} d\gamma$$

Since  $v|_{\Sigma} = 0$ ,  $\Delta v''_{\alpha\alpha} = 0$  and  $\partial v''_{\alpha\alpha}/\partial n|_{\Sigma} = 0$ , we also have

$$\int_{\Omega} \nabla v \nabla v''_{\alpha\alpha} dx = 0 \quad (54)$$

Thus

$$J''_{\lambda\lambda} = 2 \int_{\Omega} |\nabla v'_{\alpha}|^2 dx + 4 \int_{\Sigma} \alpha \frac{\partial v'_{\alpha}}{\partial n} \frac{\partial v}{\partial n} d\gamma + \int_{\Sigma} \alpha^2 \frac{\partial |v|^2}{\partial n} d\gamma \quad (55)$$

From (38) we have  $v'_{\alpha} = -\alpha \partial v/\partial n$  and so

$$\int_{\Sigma} \alpha \frac{\partial v}{\partial n} \frac{\partial v'_{\alpha}}{\partial n} d\gamma = - \int_{\Sigma} v'_{\alpha} \frac{\partial v'_{\alpha}}{\partial n} d\gamma = - \int_{\partial\Omega} v'_{\alpha} \frac{\partial v'_{\alpha}}{\partial n} d\gamma = - \int_{\Omega} |\nabla v'_{\alpha}|^2 dx \quad (56)$$

Finally, we have

$$J''_{\lambda\lambda} = -2 \int_{\Omega} |\nabla v'_{\alpha}|^2 dx + \int_{\Sigma} \alpha^2 \frac{\partial |\nabla v|^2}{\partial n} d\gamma = 2 \int_{\Sigma} \alpha \frac{\partial v}{\partial n} \frac{\partial v'_{\alpha}}{\partial n} d\gamma + \int_{\Sigma} \alpha^2 \frac{\partial |\nabla v|^2}{\partial n} d\gamma \quad (57)$$

In the case of the flat plate,  $v = (L^2 - x_2^2)/2$ , and it is not easy to decide the sign of  $J''$ . Since  $\Sigma$  has to be periodic, we can develop  $\alpha(x)$  in a Fourier series. As we shall see in Section 4.1, since the angle of contact between  $\Sigma$  and  $S$  has to be at  $90^\circ$  degrees, we should have  $d\alpha(\pm l)/dx_1 = 0$ , and so the Fourier series expansion for  $\alpha$  is

$$\alpha(x_1) = \sum_{k=1}^{\infty} \alpha_k \cos\left(k\pi \frac{x_1}{l}\right)$$

From (38) we deduce that

$$v'_{\alpha} = L \sum_k \alpha_k \cos\left(k\pi \frac{x_1}{l}\right) \cosh\left(k\pi \frac{x_2}{l}\right) \cosh\left(k\pi \frac{L}{l}\right)$$

Thus

$$\begin{aligned} J''_{\lambda\lambda} &= \int_{-l}^l -2\alpha L^2 \frac{\pi}{l} \sum_k k \alpha_k \cos\left(k\pi \frac{x_1}{l}\right) \tanh\left(k\pi \frac{L}{l}\right) + 2 \int_{-l}^l \alpha^2 L dx \\ &= 2Ll \sum_k \alpha_k^2 \left[ -\pi \frac{L}{l} k \tanh\left(k\pi \frac{L}{l}\right) + 1 \right] \end{aligned}$$



This expression changes its sign according to whether the sign of  $-\pi(L/l)k \tanh(k\pi L/l) + 1$  is larger or smaller than unity. Summing up the above result, we have the following.

*Theorem 1.* If  $\pi L/l > z$ , the root of  $1 - x \tanh x$ , then the flat plate is a local maximum for a given area because  $J''_{\lambda\lambda} < 0$ . Otherwise the flat plate is not a local minimum of  $J$  and a better shape of the same area can be found.

*Remark 1.* The above calculation also shows that a very oscillating  $\alpha$  will not improve the drag given the plate.

*Remark 2.* A similar calculation for the semi-cylinder gives

$$J'' = 128\pi l \sum_{k \geq 1} \alpha^2(k-1)$$

Thus the semi-cylinder is also a local minimum of  $J$ .

#### 4. SEARCH FOR A NUMERICAL SOLUTION

Now we shall start to solve (23) numerically by a gradient method that will need the following: finite element discretization of the problem; calculation of the gradient of the cost function with respect to the change in  $\Sigma$ .

To discretize the domain correctly, it is better to know the general shape of  $\Sigma$  *a priori*, in particular the corners if they exist.

##### 4.1. Search for corners of $\Sigma$ and the joint $\Sigma, S$

Let us put the origin at an eventual corner of  $\Sigma$  (Figure 5). If  $v$  can be expressed as a series in polar co-ordinates  $(r, \theta)$  in the neighbourhood of the origin on  $\Sigma$ , then we have

$$v(r, \theta) = \lambda r \sin(\theta - \theta_0) + r^2 f(\theta) + o(r^2) \tag{58}$$

By the definition of  $v$ ,

$$\Delta v = f'' + 4f + O(r) = -1 \tag{59}$$

Thus

$$f = -\frac{1}{4} + \mu \sin 2(\theta - \theta'_0) \tag{60}$$

But  $v|_{\Sigma} = 0$  and  $|\partial v / \partial n|_{\Sigma} = c$  on  $\Sigma = \{r(\theta), \theta\}$  gives

$$r^2 [-\frac{1}{4} + \mu \sin 2(\theta_i - \theta'_0)] + \lambda r \sin(\theta_i - \theta_0) + o(r^2) = 0 \quad i = 1, 2 \tag{61}$$

$$2r [-\frac{1}{4} - \mu \sin 2(\theta_i - \theta'_0)] + \lambda \cos(\theta_i - \theta_0) + o(r) = \pm c \quad i = 1, 2 \tag{62}$$

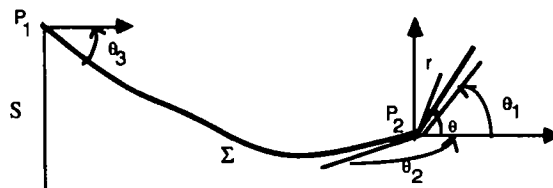


Figure 5. Study of the smoothness of  $\Sigma$

Since  $c$  is non-zero ( $-\Delta v = 1$ ,  $\partial v / \partial n |_{\partial \Omega} = 0$  is impossible), (62) implies  $\lambda \neq 0$  and so only  $\theta_1 = \theta_2 = \theta_0 \pmod{\pi}$  could make (61) zero for very small  $r$ . As a consequence, if  $v$  can be expressed in a power series of  $r$ , then  $\Sigma$  cannot have corners other than cusps.

For the contact between  $S$ ,  $\Sigma$  the same analysis gives

$$\lambda r \sin(\theta_3 - \theta_0) + o(r) = 0 \Rightarrow \theta_0 = \theta_3 \quad (63)$$

$$\lambda \cos(\pi/2 - \theta_0) + o(r) = 0 \Rightarrow \theta_0 = 0 \quad (64)$$

$$\lambda \cos(\theta_3 - \theta_0) + o(r) = \pm c = \lambda = \pm c \quad (65)$$

Thus the junction  $S$ ,  $\Sigma$  has an angle  $\pi/2$ .

#### 4.2. Discretization of (23)

Let  $\{T_h\}_h$  be a family of triangulation of  $\Omega$ , indexed by the size of the largest edge of the element, i.e. a set of triangles  $T_k$  with the following properties:

- (a)  $T_k \cap T_l = \emptyset$  or one edge or one vertex ( $k \neq l$ ).
- (b)  $\Omega_h = \cup T_k$ ;  $\partial \Omega_h$  and  $\partial \Omega$  have the same corners.
- (c) No triangle should have an angle which tends to zero or  $\pi$  when  $h$  tends to zero.

Let  $V_h$  be the space of interpolation functions of degree unity are zero-valued on  $\Sigma_h$ :

$$V_h = \{w_h \text{ continuous, affine on } T_k \forall k, \text{ zero on } \Sigma_h\} \quad (66)$$

Let  $v_h \in V_h$  be a solution of

$$\int_{\Omega_h} \nabla v_h \nabla w_h \, dx = \int_{\Omega_h} w_h \, dx \quad \forall w_h \in V_h \quad (67)$$

Now (23) in discrete form becomes

$$\max_{\Sigma_h \in \mathcal{W}} \left\{ \frac{1}{|\Omega_h|} \int_{\Omega_h} |\nabla v_h|^2 \, dx : v_h \text{ solution of (67)} \right\} \quad (68)$$

*Proposition 4.* Problem (68) has at least one solution. There exists a subsequence of a sequence of solutions of (68) which converges to a solution of (23) when  $h$  tends to zero.

*Proof.* See Reference 4, Theorem 8, p. 120.

#### 4.3. Computation of discrete gradients

Problem (68) is an optimization problem involving the positions of the vortices  $\{q^i\}_{1 \dots N}$  of the triangulation:

$$\max_{\{q^i\} \in \mathcal{Q}} \left\{ J(q^1 \dots q^N) = \frac{1}{|\Omega_h|} \int_{\Omega_h} |\nabla v_h|^2 \, dx : v_h \text{ solution of (67)} \right\} \quad (69)$$

Now the problem is to calculate the partial derivative of  $J$  with respect to  $q^i \in \mathcal{Q}$ , where  $\mathcal{Q}$  is a set of admissible positions of vertices. We proceed in two steps by considering  $J$  as a composite function of  $\{q^i\}$  with

$$v_i = v_h(q^i) \quad \forall q^i \notin \Sigma_h \quad (70)$$

In fact, if  $M$  is the number of vertices not on  $\Sigma_h$  and  $N$  is the total number of vertices, we have

$$J(q^1 \dots q^N) = E(q^1 \dots q^N, v_1 \dots v_M) \quad (71)$$

and so

$$\frac{\partial J}{\partial q_j^i} = \frac{\partial E}{\partial q_j^i} + \sum_{l=1 \dots M} \frac{\partial E}{\partial v_l} \frac{\partial v_l}{\partial q_j^i} \quad (72)$$

There are two advantages in this procedure (introduced in Reference 7):

1. It reflects the method of programming (69); in general,  $J$  is calculated by a subroutine with  $\{q^i\}$  and  $\{v_i\}$  as parameters.
2. It allows the cost function to be changed very easily. (We will use this characteristic later.)

The partial derivatives  $\partial E/\partial q_j^i$  and  $\partial E/\partial v_l$  have been calculated by the finite difference technique as

$$\frac{\partial E}{\partial q_j^i} \approx \frac{E(q^1 \dots q^i + e^j \delta q \dots q^N, v_1 \dots v_M) - E(q^1 \dots q^N, v_1 \dots v_M)}{\delta v} \quad (73)$$

$$\frac{\partial E}{\partial v_l} \approx \frac{E(q^1 \dots q^N, v_1 \dots v_l + \delta v \dots v_M) - E(q^1 \dots q^N, v_1 \dots v_M)}{\delta v} \quad (74)$$

where  $e^j$  is the  $j$ th basis vector of the orthogonal system  $(0x_1, 0x_2)$ . To calculate  $\partial v_l/\partial q_j^i$ , we proceed as in Reference 4. By differentiating (67), we have

$$\int_{\delta \Omega_h} \nabla v_h \nabla w_h \, dx + \int_{\Omega_h} \nabla \delta v_h \nabla w_h \, dx + \int_{\Omega_h} \nabla v_h \nabla \delta w_h \, dx = \int_{\Omega_h} \delta w_h \, dx + \int_{\delta \Omega_h} w_h \, dx \quad (75)$$

where the  $\delta$  are the variations due to the displacement of the vertex  $q^i$  in the direction  $e^i$ , and  $\delta w_h$  is the change in the basis of  $V_h$  which is given by Proposition 2 of Reference 4. (p. 102) as

$$\delta w_h = - \frac{\partial w_h}{\partial x_j} w^i \delta q \quad (76)$$

From Proposition 3 of Reference 4 (p. 102) we have

$$\int_{\delta \Omega_h} f(x) \, dx = \sum_{\{k: T_k \supset \{q\}\}} \int_{T_k} \delta q \frac{\partial (f(x) w^i)}{\partial x_j} \, dx \quad (77)$$

so

$$\int_{\delta \Omega_h} \nabla v_h \nabla w_h \, dx = \sum_{\{k: T_k \supset \{q\}\}} \int_{T_k} \delta q \frac{\partial w^i}{\partial x_j} \nabla v_h \nabla w_h \, dx$$

and

$$\int_{\delta \Omega_h} w_h \, dx = \sum_{\{k: T_k \supset \{q\}\}} \int_{T_k} \delta q \frac{\partial (w^i w_h)}{\partial x_j} \, dx$$

Using the above expressions, we can rewrite (75) as

$$\int_{\Omega_h} \nabla \delta v_h \nabla w^i \, dx = \delta q \chi_{ij}^i \quad (78)$$

with

$$\chi_{ij}^i = \sum_{\{k: T_k \supset \{q\}\}} \int_{T_k} \left( \frac{\partial (w^i w^i)}{\partial x_j} - \frac{\partial w^i}{\partial x_j} \nabla v_h \nabla w^i + \nabla w^i \nabla w^i \frac{\partial v_h}{\partial x_j} - \frac{\partial w^i}{\partial x_j} w^i \right) dx$$

where  $w^l$  is a canonical basis function of  $V_h$  associated with  $q^l$  and is defined by

$$w^l(q^k) = \delta_{kl} \quad w^l \in V_h \quad (79)$$

As is usual in the theory of optimal control, we do not need to know  $\partial v_l / \partial q_j^i$  but only how to calculate the expression (72). So we introduce the adjoint state function  $p_h \in V_h$  defined by

$$\int_{\Omega_h} \nabla p_h \nabla w^l \, dx = \partial E / \partial v_l \quad l = 1 \dots M \quad (80)$$

From (71)

$$v_h(x) = \sum v_k w^k(x) \quad (81)$$

and we get

$$\delta v_h = \delta q \sum_k \frac{\partial v_k}{\partial q_j^i} w^k + \sum_k v_k \delta w^k \quad (82)$$

From (76) we have

$$\delta w^k = - \delta q w^i \frac{\partial w^k}{\partial x_j} \quad (83)$$

and thus by letting

$$v_h^i = \sum_k \frac{\partial v_k}{\partial q_j^i} w^k \quad (84)$$

we get from (78)

$$\int_{\Omega_h} \nabla v_h^i \nabla w^l \, dx = \chi_{ij}^l \quad (85)$$

with

$$\chi_{ij}^l = \chi_{ij}^l + \int_{\Omega_h} \frac{\partial v_h}{\partial x_j} \nabla w^i \nabla w^l \, dx$$

From equations (80) and (85) we calculate

$$\sum_l \frac{\partial E}{\partial v_l} \frac{\partial v_l}{\partial q_j^i} = \sum_l \int_{\Omega_h} \nabla p_h \nabla \left( w^l \frac{\partial v_l}{\partial q_j^i} \right) \, dx = \int_{\Omega_h} \nabla v_h \nabla p_h \, dx = \sum_l p_l \chi_{ij}^l \quad (86)$$

where

$$p_l = p_h(q^l) \quad (87)$$

Let us sum up the above results in the following proposition.

*Proposition 5.*

$$\frac{\partial J}{\partial q_j^i} = \frac{\partial E}{\partial q_j^i} + \sum_l p_l \chi_{ij}^l \quad (88)$$

where  $J$  is related to  $E$  by (71),  $p_l$  is defined by (80), (87) and  $\chi_{ij}^l$  by (79), (85).

#### 4.4. Description of the set of admissible positions $Q$

In the optimization algorithm we start with an initial shape and then deform it iteratively to get an optimal shape. In this process, when boundary nodes are moved, the internal nodes should also be moved in such a way as to keep the triangulation reasonable. There are two possibilities:

- (a) The internal nodes  $q^i$  may be allowed to move freely in proportion to  $\partial J/\partial q_j^i$  and only the step size of the gradient method must be limited to avoid the overlapping of the triangles.
- (b) The internal nodes  $q^i$  may be related to the boundary nodes  $\{q^j\}$  by a formula of the type

$$q^i = Q^i(\{q^j\}) \quad (89)$$

Here we use the second method in the optimization. To keep (27) ( $|\Omega| = a$ ), we have to have

$$\int_{\Sigma_h} x_2 \, d\gamma = a = \sum_{\{j: q_j \in \Sigma_h\}} \frac{(q_2^{j+1} + q_2^j)(q_1^{j+1} - q_1^j)}{2} \quad (90)$$

Finally, we make the first and last nodes of  $\Sigma$  stay on  $S$ , i.e. the nodes move vertically and  $\Sigma$  should lie within the region limited by  $S$ .

#### 4.5. A gradient method

Without (90), the constraints on  $\{q^i\}$  are box constraints which will not be active near the solution and which can be taken care of only by limiting the step size  $\rho^n$  of the gradient algorithm. The constraint (90) becomes linear when  $w_j = (q_1^{j+1} - q_1^j)/2$  remains constant in the optimization algorithm, which is the case if the nodes are restricted to move vertically. Thus we can now use a projected gradient method only with respect to the nodes on  $\Sigma$ .

Let  $\{q^j; j \in K\}$  be the vertices on  $\Sigma$ . From (89) we deduce

$$\delta q^i = \sum_{j \in J} \frac{\partial Q^i}{\partial q_2^j} \delta q_2^j \quad \forall i \notin K \quad (91)$$

and so with (91) we can express the variations of the cost function as variations with respect to vertices on  $\Sigma$  only. Proposition 5 and (91) allow us to calculate  $\xi_j$  such that

$$\delta J = \sum_{j \in J} \xi_j \delta q_2^j \quad (92)$$

If we differentiate (90), we get a relation of the type

$$\sum_{j \in J} w_j \delta q_2^j = 0 \quad (93)$$

and consequently the projected gradient of  $J$  with respect to  $q^j$  becomes

$$J'_{,j} = \xi_j - \frac{\sum_{j \in J} \xi_j w_j}{\sum_{j \in J} w_j^2} w_j \quad (94)$$

Therefore the main loop of the gradient algorithm is

$$q^{j,n+1} = q^j(\rho^n) \quad \text{with } q_2^j(\rho) = q_2^j + \rho^n J'_{,j}, \quad q_1^j(\rho) = q_1^j \quad (95)$$

where  $\rho^n$  maximizes  $J(q^i(\rho))$  subject to the box constraints. The internal nodes are functions

of  $\rho$  and therefore from (91) are constructed by

$$q^i(\rho) = q^{i,n} + \sum_{j \in J} \frac{\partial Q^i}{\partial q^j} (q^j(\rho) - q^{j,n}) \quad \forall i \notin K \quad (96)$$

## 5. NUMERICAL RESULTS

### 5.1. Resolution of (23)–(27)

We first solve problem (23) with area constraint (27) by the projected gradient method explained in Section 4. To avoid oscillations of the free boundary  $\Sigma$ , we do not allow all points of  $\Sigma$  to move independently but only the odd ones. The even points are constrained to be in the middle of their two neighbouring odd ones:

$$q^{2p} = \frac{l_2 q^{2p-1} + l_1 q^{2p+1}}{l_1 + l_2} \quad (97)$$

where  $l_1 = |q^{2p} - q^{2p-1}|$ ,  $l_2 = |q^{2p+1} - q^{2p}|$ ,  $p = 1, 2, \dots$ . As before, the odd nodes are moved vertically only. Naturally we have to take (97) into account in the computation of the gradients of  $J$ , and this has been done in the same manner as we did in (93).

The results of the optimization are given in Figures 6 and 7 (convergence of the domain,

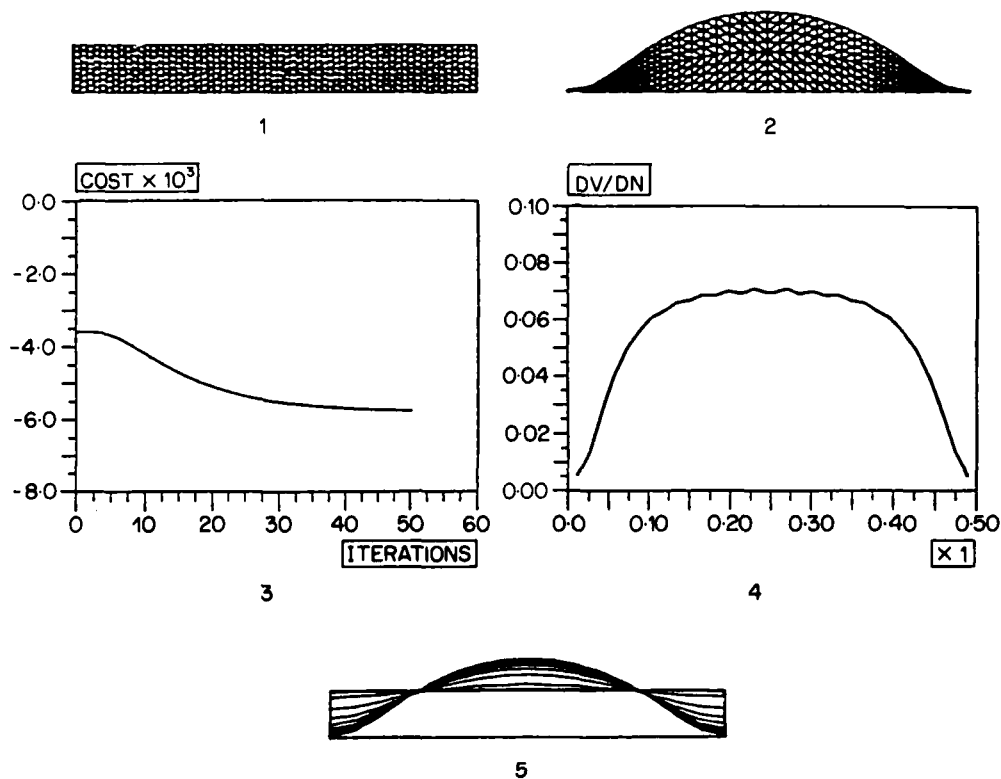


Figure 6. Results after 60 iterations starting from the domain shown in 1 ( $L = 0.06$ ,  $l = 1/2$ ). The cost function  $\int_{\Omega} |\nabla v|^2 dx$  has initial value  $= 0.36 \cdot 10^{-4}$  and final value  $= 0.58 \cdot 10^{-4}$ . Figure 2 shows the shape of iteration 60; Figure 3 the values of the cost function at each iteration, Figure 4 the value of  $\partial v / \partial n$ ; and Figure 5 shows some intermediate shapes

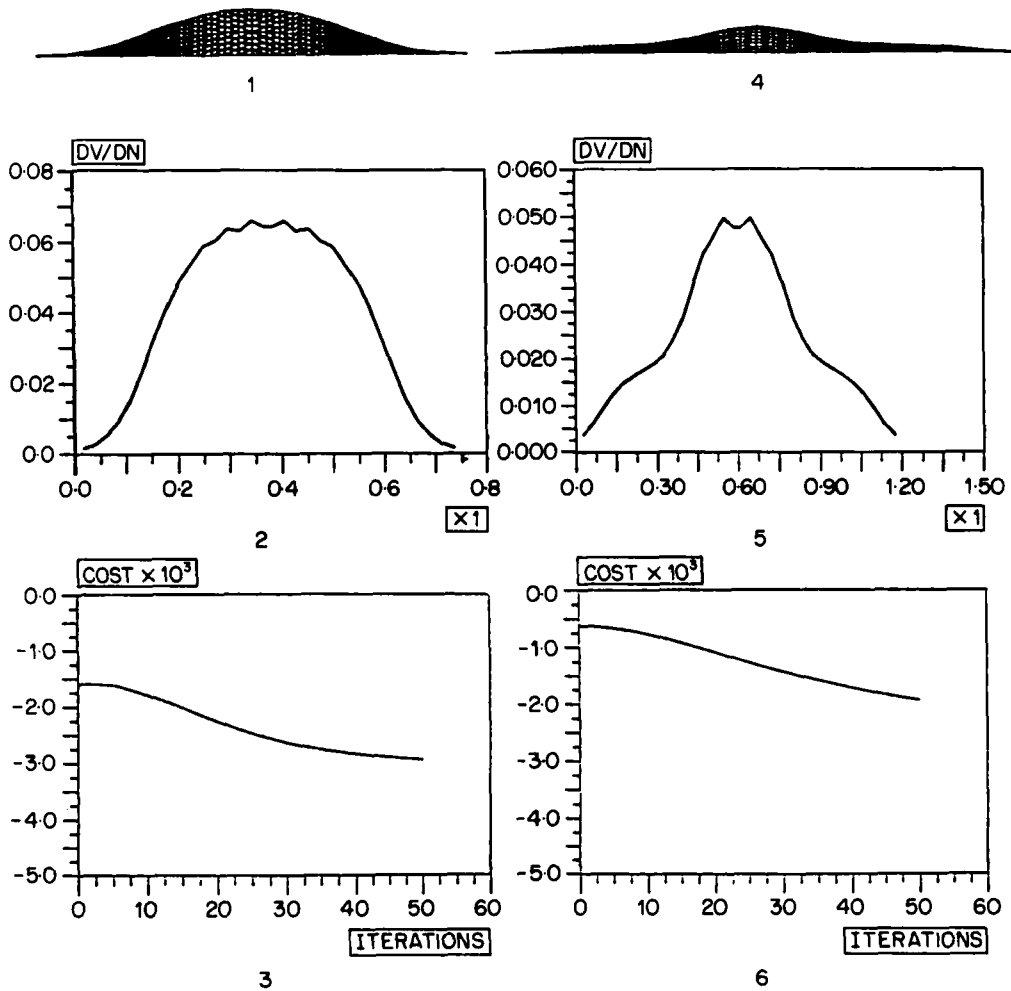


Figure 7. Same as figure 6 but with 2 other widths: Figure 1:  $L = 0.04$ ,  $l = 3/4$ ;  $\partial v/\partial n$  versus  $x_1$  and  $J$  versus  $n$  are shown on 2 and 3.  $J_{60} = 0.29 \times 10^{-4}$ , result on Figure 1. Figure 4:  $L = 0.025$ ,  $l = 1.2$ ;  $\partial v/\partial n$  versus  $x_1$  and  $J$  versus  $n$  are shown on 5 and 6.  $J_{60} = 0.6 \times 10^{-3}$ , result on Figure 4

relation between  $\partial v/\partial n$  and  $\Sigma$ ). In this process we have also verified that the approximations (73) and (74) are correct: when one vertex moves up from the flat plate  $|\partial J/\partial q|$  is analytically equal to  $0.444639 \times 10^{-3}$ , while the finite difference subroutine gives  $0.444640 \times 10^{-3}$ .

Thus three cases have been computed, each with the same area  $0.03$ . In the first case the riblet width is  $0.5$ ; after 60 iterations a shape is obtained (Figure 6) with drag equal to

$$\frac{d}{2} \nu \frac{|\Omega|}{J_{60}} = d\nu \frac{0.03 \times 10^4}{2 \times 0.58} = 250 d\nu$$

giving a drag per unit width of  $500 d\nu$ . This should be compared with the drag per unit width of a flat plate, which is equal to  $834 d\nu$ . In the second case (Figure 7) the riblet width is  $0.75$ , which gives a drag equal to  $520 d\nu$  and a drag per unit width of  $600 d\nu$ . Finally, in the third case (Figure 7) the width is  $1.2$ , the drag is  $790 d\nu$  and the drag per unit width is  $660 d\nu$ . Therefore the first shape (Figure 6) is the best.

5.2. Reformulation of the problem

When  $L \ll l$  (thin boundary layer), the optimality conditions are not very well satisfied by the shape found numerically (Figure 7). We might ask whether we are in the numerical noise of the discretization or whether the discrete shape is very far from the continuous solution even though there is convergence of the cost function to a plateau. To improve the result, since the optimality conditions are known ( $|\nabla v| = \text{constant}$  on  $\Sigma$ ), we have the problem

$$\min_{\Sigma \in W} \left\{ \int_{\Sigma} (|\nabla v|^2 - \langle \nabla v|^2 \rangle)^2 d\gamma : v \text{ solution of (18)} \right\} \quad (98)$$



Figure 8. Starting from one of the forms of Figure 6 and searching for solutions satisfying  $\partial v / \partial n = \text{constant}$ , the flat plate is found when problem (99) is solved

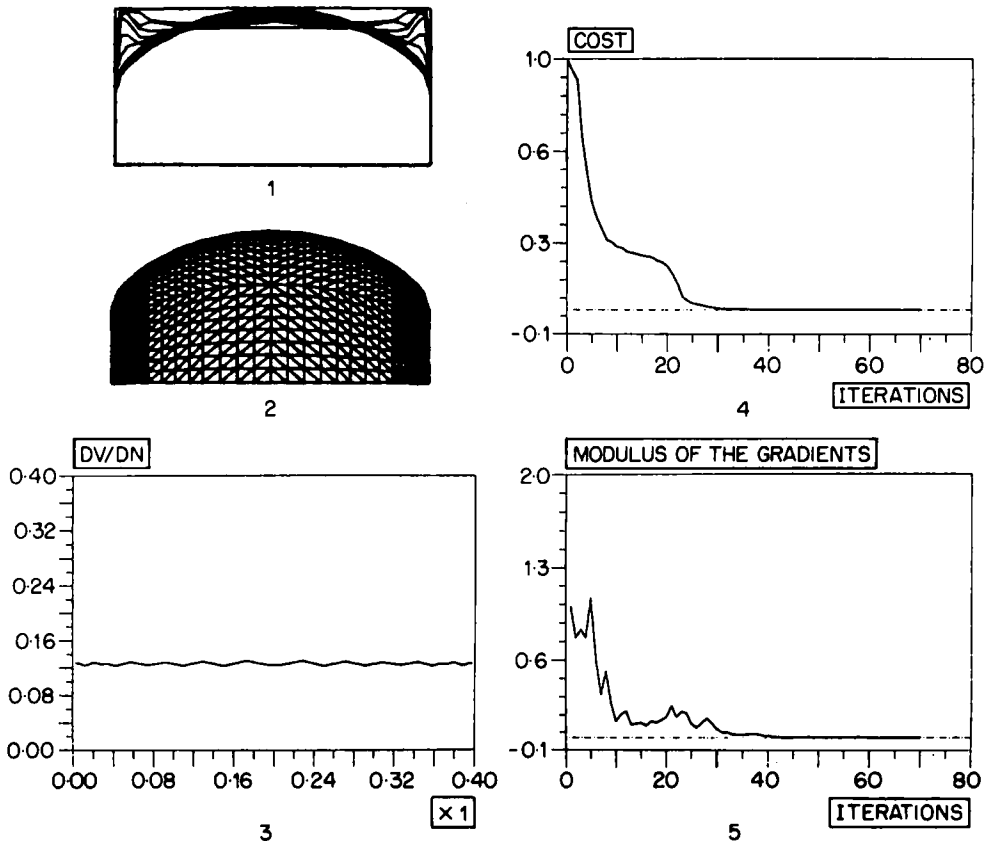


Figure 9. Problem (101) is solved with  $c/L^2 = 2/5$ . On Figure 1: intermediate shapes; on Figure 2: final shape; on Figure 3:  $\partial v / \partial n$  on the final shape versus  $x_1$ ; on Figure 4: values of  $J$  versus iteration number; on Figure 5: gradient of  $J$  versus iteration number.



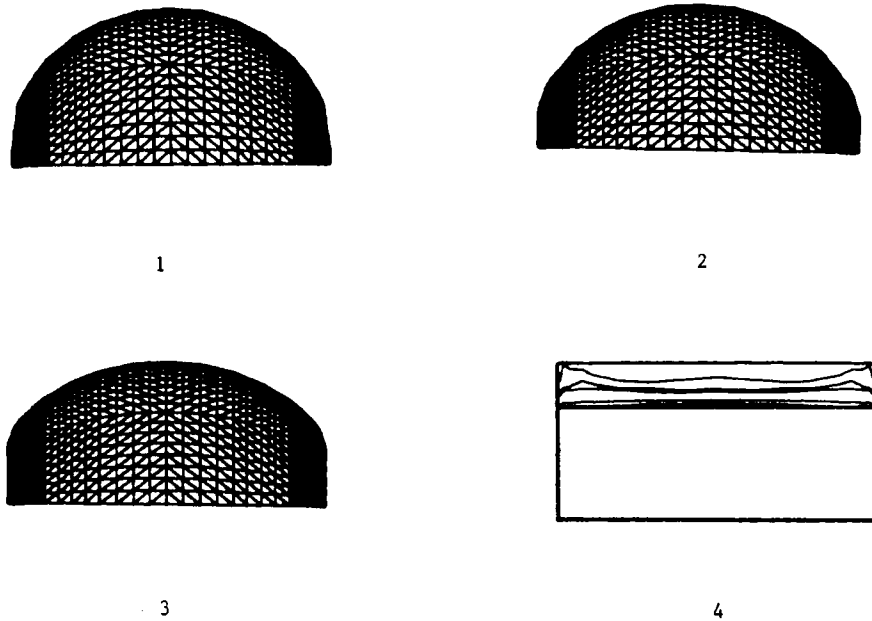


Figure 9b. Other solutions of (101) with different values of  $c/L^2$ . The fourth shape is the flat plate and so intermediate shapes are shown.

	$c/L^2$	$\partial v/\partial n$	$\int_{\Omega}  \nabla v ^2 /  \Omega $	$ \Omega $
Figure 1	1/4	0.11	$5.0 \cdot 10^{-3}$	0.064
Figure 2	2/7	0.12	$5.1 \cdot 10^{-3}$	0.059
Figure 3	1/3	0.13	$6.0 \cdot 10^{-3}$	0.061
Figure 4	1/2	0.14	$6.8 \cdot 10^{-3}$	0.057
Figure 9a	2/5	0.13	$7.4 \cdot 10^{-3}$	0.067

or in the discrete version

$$\min_{\Sigma_h \in W} \left\{ \int_{\Sigma_h} (|\nabla v_h|^2 - \langle |\nabla v_h^2| \rangle)^2 d\gamma : v_h \text{ solution of (67)} \right\} \tag{99}$$

where  $\langle \rangle$  denotes the average over  $\Sigma$ :

$$\langle |\nabla v|^2 \rangle = \frac{\int_{\Sigma} |\nabla v|^2 d\gamma}{\int_{\Sigma} d\gamma} \tag{100}$$

This problem has been solved in exactly the same way as for (23), and the modifications in the program were minimal because of (72)–(74) (see Figure 8). However, the results are disappointing because the flat plate seems to be the absolute minimum of (99).

We have therefore considered a third type of problem

$$\min_{\Sigma \in W'} \left\{ \int_{\Sigma} (|\nabla v|^2 - c^2)^2 d\gamma : v \text{ solution of (18)} \right\} \tag{101}$$

where  $W'$  does not have any constraints on  $|\Omega|$  except the given surface area  $a$ . On varying  $c$ , we obtain some curves  $\Sigma$  on which  $\partial v/\partial n$  is nearly constant and which lie between a semi-cylinder and flat plate. But here again it seems that the new curves have maximum drag (see Figure 9). We remark that the joints  $S-\Sigma$  do not conform with the theory in Section 4.1. This

is probably due to the numerical singularity created by the transition from the Newman to the Dirichlet condition at the corner.

## 6. CONCLUSIONS

The problem of optimizing riblets (to reduce the drag of the quasi-planar surfaces in a uniform flow) is remarkable in the sense that the theory of optimal design suits this problem well. We have obtained an existence result, first-order and second-order optimality conditions and a preliminary analysis of eventual singularities. The theory indicates that the flat plate is optimal when the laminar boundary layer is thick with respect to the distance between two riblets, but is not optimal when it is thin with respect to the distance between two riblets. Since this distance is arbitrary, the analysis shows, in fact, that the flat plate can never be optimal and the riblets given in Figure 6 (the best we have found) reduce the drag. However, the drag reduction by both shapes is about the same, namely 15%; this value seems large, but it should be remembered that this is a Poiseuille flow analysis. These shapes have been obtained numerically by the finite element method coupled with a gradient optimization algorithm.

This study assumes that the riblet problem is a problem in the laminar boundary layer and that the thickness of this laminar boundary, on average, is constant, irrespective of the shape of the riblets. These two hypotheses remain to be verified experimentally or by a numerical simulation using the full Navier–Stokes equations.

## ACKNOWLEDGEMENTS

We thank Prof. P. Perrier and Prof. J. Cousteix for important discussions on the modelling of the problem.

## APPENDIX I: NOTATION

$\nu$	reduced viscosity of the fluid
$p$	pressure of the fluid
$u$	velocity of the fluid parallel to the body
$\Sigma$	boundary of riblets
$\Omega$	two-dimensional domain of calculation of $u$
$\partial\Omega$	boundary of $\Omega$
$S$	$= \partial\Omega - \Sigma$
$W$	a set of admissible forms for $\Sigma$
$ \Omega $	area of $\Omega$
$d$	fluid flux through $\Omega$ (see equation (13))
$k$	pressure gradient in the direction parallel to the body
$D$	drag of $\Sigma$
$v$	$= u/k$ , auxiliary velocity used to reformulate the problem

## APPENDIX II

Let us calculate the second derivative of

$$\int_{\Omega} f(x, y) \, dx \, dy$$

when

$$\Omega = \{(x, y) : -l \leq x \leq l; 0 \leq y \leq L(x)\}$$

is replaced by

$$\Omega' = \{(x, (1 + \beta(x))y) : (x, y) \in \Omega\}$$

We have

$$\begin{aligned} \int_{\Omega'} f(x, y) \, dx \, dy &= \int_{\Omega} f(x, y(1 + \beta(x)))(1 + \beta(x)) \, dx \, dy \\ &= \int_{\Omega} f(x, y) \, dx \, dy + \int_{\Omega} \beta(x)(f + yf'_{,y}) \, dx \, dy + \int_{\Omega} \beta^2(x) \left( f'_{,y}y + f'_{,yy} \frac{y^2}{2} \right) \, dx \, dy \end{aligned}$$

But

$$\int_{\Omega} \beta y f'_{,y} \, dx \, dy = \int_{-l}^l \beta \, dx \int_0^L y f'_{,y} \, dy = \int_{-l}^l L f(x, L(x)) \beta(x) \, dx - \int_{\Omega} f \beta \, dx \, dy$$

and

$$\frac{1}{2} \int_{-l}^l \beta^2 f'_{,yy} y^2 \, dx \, dy = \int_{-l}^l \beta^2 \left( f'_{,y}(x, L(x)) \frac{L(x)^2}{2} - \int_0^L f'_{,y} y \, dy \right) \, dx$$

Thus

$$\int_{\Omega'} f \, dx = \int_{\Omega} f \, dx + \int_{\Sigma} f L \beta \, d\gamma + \int_{\Sigma} \frac{(\beta L)^2}{2} f'_{,y} \, d\gamma$$

which implies, when  $\lambda \alpha = L\beta$  and  $\Omega$  is a rectangle,

$$\frac{d^2}{d\lambda^2} \int_{\Omega} f \, dx = \int_{\Sigma} \alpha^2 \frac{\partial f}{\partial n} \, d\gamma$$

#### REFERENCES

1. Walsh, M., 'Drag characteristics of V-groove and transverse curvature riblets', *Proc. Symp. on Viscous Drag Reduction*, Dallas, TX, November 1979.
2. Cea, J. and E. J. Haug, (eds) *Optimization of Distributed Parameter Structures*, Alphen aan der Rijn, Amsterdam, 1981.
3. Murat, F. and J. Simon, 'Studies in optimal shape design problem', in Cea, J. (ed.), *Lecture Notes in Computer Sciences, Vol. 41*, Springer, 1976.
4. Pironneau, O., 'Optimal shape design for elliptic systems', *Springer Lecture Notes in Computational Physics*, Springer, New York, 1984.
5. Zolezio, J. P., 'The material derivative method for optimal shape design problems', in Cea, J. and E. J. Haug (eds), *Optimization of distributed parameter structures*, Alphen aan der Rijn, Amsterdam, 1981.
6. Chenais, D., 'On the existence of solution in a domain identification problem,' *J. Math. Anal. Appl.*, **52** (2), (1975).
7. Arumugan, G. and O. Pironneau, 'Towards a multipurpose optimal shape design computer code', IFIP workshop W.T.7, Nice, Jan. 1987 (to appear).